THE JOURNAL OF BIOLOGICAL CHEMISTRY VOL. 287, NO. 41, pp. 34583–34595, October 5, 2012

Ezrin/Radixin/Moesin Are Required for the Purinergic P2X7 Receptor (P2X7R)-dependent Processing of the Amyloid Precursor Protein*

Received for publication, July 11, 2012, and in revised form, August 8, 2012 Published, JBC Papers in Press, August 13, 2012, DOI 10.1074/jbc.M112.400010

Amaria Darmellah[‡1,2], **Amel Rayah**[‡1,3], **Rodolphe Auger**[‡], **Marie-Hélène Cuif**[§], **Magali Prigent**[§], **Monique Arpin**[¶], **Andres Alcover**[‖], **Cécile Delarasse**[**4], **and Jean M. Kanellopoulos**[‡5]

From the [‡]*Institut de Biochimie et Biophysique Moléculaire et Cellulaire, CNRS UMR 8619 and* [§]*Institut de Génétique et Microbiologie, CNRS UMR 8621, Université Paris Sud, 91405 Orsay Cedex, France,* [¶]*Centre de Recherche, Institut Curie, CNRS UMR 144, 75248 Paris, France,* [‖]*Lymphocyte Cell Biology Unit, Department of Immunology, Institut Pasteur, CNRS URA1961, 75015 Paris, France, and* **Centre de Recherche, Institut du Cerveau et de la Moelle Épinière, INSERM UMRS_975, Université Pierre et Marie Curie (Paris 6), CNRS UMR 7225, 75013 Paris, France*

Background: The purinergic receptor P2X7, an ATP-gated cation channel, triggers the proteolytic cleavage of membrane glycoproteins by α-secretases.
Results: P2X7R induces ezrin, radixin, and moesin (ERM) phosphorylation, which activates the proteolytic cleavage of the amyloid precursor protein (APP).
Conclusion: ERM phosphorylation is required for the P2X7R-dependent release of the neuroprotective fragment of APP.
Significance: ERM can control the non-amyloidogenic processing of APP.

The amyloid precursor protein (APP) can be cleaved by α-secretases in neural cells to produce the soluble APP ectodomain (sAPPα), which is neuroprotective. We have shown previously that activation of the purinergic P2X7 receptor (P2X7R) triggers sAPPα shedding from neural cells. Here, we demonstrate that the activation of ezrin, radixin, and moesin (ERM) proteins is required for the P2X7R-dependent proteolytic processing of APP leading to sAPPα release. Indeed, the down-regulation of ERM by siRNA blocked the P2X7R-dependent shedding of sAPPα. We also show that P2X7R stimulation triggered the phosphorylation of ERM. Thus, ezrin translocates to the plasma membrane to interact with P2X7R. Using specific pharmacological inhibitors, we established the order in which several enzymes trigger the P2X7R-dependent release of sAPPα. Thus, a Rho kinase and the MAPK modules ERK1/2 and JNK act upstream of ERM, whereas a PI3K activity is triggered downstream. For the first time, this work identifies ERM as major partners in the regulated non-amyloidogenic processing of APP.

The amyloid precursor protein (APP)[6] can be processed by three different proteases, α-, β-, and γ-secretases, which are able to cleave APP at different sites (1, 2). The amyloid β peptides produced by β- and γ-secretases are present in senile plaques of patients with Alzheimer disease. In contrast, α-secretases cleave APP within the amyloid β peptide sequence, precluding the formation of neurotoxic peptides and generating the soluble APP ectodomain (sAPPα) endowed with neuroprotective properties (3). Recently, we have demonstrated that P2X7 receptor (P2X7R) stimulation triggers the proteolytic cleavage of APP leading to the shedding of sAPPα from various neural cells (4).

The P2X7R belongs to the P2X receptor family of ATP-gated cation channels. Brief activation of P2X7R with extracellular ATP in its tetra-anionic form, ATP^{4-}, opens cation-specific ion channels. Prolonged ligation of P2X7R results in the formation of non-selective membrane pores permeable to molecules of molecular mass up to 900 Da. Depending on the cell type, P2X7R stimulation triggers different pores that allow cationic and anionic dye uptake in macrophages but only cationic dyes in HEK293 cells (5). Prolonged ATP ligation of P2X7R can lead to membrane blebbing (6) and cell death by apoptosis (7) or lysis/necrosis (8, 9) depending on the cell type. The physiological significance of cell death mediated by P2X7R stimulation remains to be determined. Recent evidence also suggests that P2X7R may in some conditions trigger growth or promote survival (10). Indeed, Adinolfi *et al.* (11) identified a shorter P2X7R natural splice variant lacking the C-terminal region that can heterotrimerize with the longer P2X7R isoform. Their results suggest that if the longer isoform is predominant in the heterotrimer P2X7R will stimulate the non-selective pore opening

* This work was supported in part by the CNRS and Agence Nationale pour la Recherche Grant ANR-07-BLAN-0089-02.
[1] Both authors contributed equally to this work.
[2] Supported by a postdoctoral fellowship from Neuropôle de Recherche Francilien.
[3] Supported by a Ph.D. fellowship from the French government.
[4] Supported by Association France Alzheimer. To whom correspondence may be addressed: CRICM, INSERM UMRS_975, Université Pierre et Marie Curie (Paris 6), CNRS UMR 7225, 75013 Paris, France. E-mail: cecile.delarasse@upmc.fr.
[5] Supported by Association France Alzheimer. To whom correspondence may be addressed. Tel.: 33-1-69-15-46-88; Fax: 33-1-69-85-37-15; E-mail: jean.kanellopoulos@u-psud.fr.
[6] The abbreviations used are: APP, amyloid precursor protein; Ab, antibody; Bz-ATP, benzoylbenzoyl ATP; FERM, band Four point one ezrin, radixin, moesin; ERM, ezrin, radixin, and moesin; EtBr, ethidium bromide; P2X7R, P2X7 receptor; sAPPα, soluble APP ectodomain; MAP, mitogen-activated protein; ANOVA, analysis of variance; NHERF, sodium-hydrogen exchanger regulatory factor; ADAM, a disintegrin and metalloproteinase; DiI, 1,1′-Dioctadecyl-3,3,3′,3′-Tetramethylindocarbocyanine Perchlorate.

leading to cell death. In contrast, if the shorter isoform is in excess, P2X7R will trigger cell growth (11).

In addition to its role in cell death/proliferation, numerous physiological functions have been attributed to P2X7R, notably activation of caspase-1 (12, 13), rapid release of mature IL-1β from macrophages (14, 15), and killing of various intracellular pathogens in macrophages (16, 17). Moreover, P2X7R activation triggers the proteolytic cleavage of plasma membrane proteins such as L-selectin, CD23, TNFα, CD27, matrix metalloproteinase-9, and interleukin-6 receptor (18–22).

P2X7R stimulation leads to rapid plasma membrane blebbing (23). Furthermore, it has been shown that ezrin, radixin, and moesin (ERM) are involved in cell cortex rigidity that may control membrane blebbing associated to some cellular processes (24). ERM are considered as key cell cortex organizers, being involved in a variety of major cellular functions like cell shape regulation, cell adhesion and motility, protein subcellular localization, intracellular vesicle traffic, and receptor signal transduction (for reviews, see Refs.25–28). It is currently accepted that ERM can interact with a wide variety of cellular components, including adhesion receptors, ion channels, signaling effectors, and vesicle traffic regulators (28–36). ERM also ensure the interactions between the cortical actin cytoskeleton and microtubule networks (37, 38). ERM proteins link actin filaments to plasma membrane components directly via the cytosolic region of membrane receptors or indirectly through scaffolding proteins bound to transmembrane proteins (26, 39), including substrates for metalloproteases (40). In the cytosol, ERM proteins exist in a closed conformation due to intramolecular interactions between the N- and C-terminal domains masking the membrane and F-actin binding sites (for reviews, see Refs. 26 and 39). Activation of ERM is triggered by sequential binding of the N-terminal domain to phosphatidylinositol 4,5-bisphosphate and phosphorylation of a conserved threonine residue (Thr-567 in ezrin) (41). After unfolding, ERM bind to the cytoplasmic domain of numerous transmembrane proteins such as CD44, CD43, L-selectin, and ICAM-2 and link them to F-actin (40). Thus, we determined whether P2X7R stimulation triggers ERM activation and to what extent ERM control P2X7R-mediated cellular functions, including the activation of some plasma membrane proteases.

In the present studies, we demonstrated that P2X7R activation leads to ERM phosphorylation and that these proteins are required for the non-amyloidogenic cleavage of APP. In addition, we found that P2X7R and ERM interact after P2X7R activation. Therefore, ERM are key components in the biochemical pathway leading to sAPPα shedding following P2X7R stimulation.

EXPERIMENTAL PROCEDURES

Animals—Four- to 8-week-old C57BL/6 mice were purchased from Charles River Laboratories. P2X7R-deficient mice, backcrossed to C57BL/6 mice for seven generations, were from The Jackson Laboratory (Bar Harbor, ME).

Reagents and Antibodies—DMEM and DMEM/F-12 were obtained from Invitrogen. ATP and benzoylbenzoyl ATP (Bz-ATP) were from Sigma-Aldrich. Nerve growth factor (NGF) was from Alomone Labs (Jerusalem, Israel). U0126, U0124, SP600125, fasudil, wortmannin, and LY294002 were from Calbiochem. A438079, a selective antagonist of P2X7R, was obtained from Tocris Bioscience (Bristol, UK).

The following antibodies (Abs) were used for immunofluorescence and Western blotting: unconjugated mouse monoclonal antibody (mAb) anti-human APP clone 22C11 (Chemicon, Temecula, CA); affinity-purified rabbit anti-P2X7R Abs recognizing residues 576–595 of P2X7R (Alomone Labs); rabbit anti-extracellular signal-regulated kinase 1/2 (ERK1/2) (Thr(P)-202/Tyr(P)-204), anti-c-Jun N-terminal kinase (JNK)/SAPK (Thr(P)-183/Tyr(P)-185), and rabbit anti-phospho-ERM (Thr-567/Thr-564/Thr-558) antibodies (Cell Signaling Technology, Danvers, MA); and rabbit anti-ERK1/2, anti-JNK/SAPK, anti-ezrin, and anti-ERM Abs (Cell Signaling Technology). Affinity-purified goat anti-rabbit IgG Abs coupled to peroxidase (Rockland Immunochemicals, Gilbertsville, PA), goat anti-mouse IgG Abs coupled to peroxidase, and mouse mAb anti-goat/sheep IgG conjugated to peroxidase (Sigma-Aldrich) were used as secondary Abs for Western blot analyses, and goat anti-rabbit IgG Abs coupled to Alexa Fluor 488 (Invitrogen) were used as secondary Abs for immunofluorescence.

Cell Cultures—Neuro2a mouse neuroblastoma cells and HEK293 cells were maintained in DMEM containing 10% fetal calf serum (FCS). Because an excellent mAb capable of detecting human APP and its fragments exists, we have previously transfected Neuro2a cells with a plasmid encoding the V5-tagged human APP cDNA (4). Stable transfectants were cloned and used in the present work. Cultures of newborn astrocytes were prepared from the hemispheres of 1–3-day-old mice. Cells were grown as described previously (4). SK-N-BE human neuroblastoma cells were maintained in DMEM/F-12 containing 10% FCS.

Cell Stimulation—Neuro2a cells were cultured for 48 h in DMEM containing 10% FCS. Medium was then removed, and cells were incubated for 2 h in DMEM at 37 °C. Subsequently, cells were stimulated with 1 mM Bz-ATP or 100 ng/ml NGF for 15 min.

Western Blot Analyses—Proteins from cell lysates or cell supernatants were analyzed as described previously (4). Blots were immunostained with primary Ab at 4 °C overnight and probed with secondary Ab conjugated to horseradish peroxidase. Specific bands were visualized by enhanced chemiluminescence (Perkin-Elmer Life Sciences). To quantify the extent of phosphorylation of each kinase, the phosphorylated band density was expressed relative to the intensity of the total protein band.

RNA Interference and Plasmid Transfections—Neuro2a cells were stably transfected with the human APP. Small interfering RNAs (siRNAs) targeting mouse ezrin, radixin, and moesin and control siRNA were from Dharmacon (Cramlington, UK). Neuro2a cells were transfected with 1 μM siRNA using Cell Line Nucleofector Kit V (Amaxa, Gaithersburg, MD) as described by the manufacturer. Inhibition of targeted protein was confirmed by Western blot 48 h after transfection. To study ezrin translocation to the plasma membrane, we transfected Neuro2a cells with plasmids containing the cDNA encoding 1) the green fluorescent protein (GFP) pmaxGFP (Lonza), 2) the GFP fused to ezrin, or 3) the GFP fused to the N-terminal FERM domain of ezrin.

Video Microscopy—Cells were observed using a Leica DM IRE2 microscope, and images were captured by a charge-coupled device camera (10-MHz Cool SNAPHQ, Roper Instru-

ments). Metamorph software (Universal Imaging Corp.) was used to deconvolute Z-series and treat the images.

Immunofluorescence—Neuro2a cells seeded on polylysine-coated Lab-Tek slides at 2×10^4 cells/well were incubated with Vybrant DiI cell labeling solution (Molecular Probes) for 15 min and stimulated with 1 mM Bz-ATP for 10 min. Cells were fixed with 4% paraformaldehyde, nonspecific sites were blocked using PBS containing 10% BSA, and permeabilization was carried out using 0.1% saponin. Phospho-ERM were detected with rabbit anti-phospho-ERM Abs that were applied for 1 h at room temperature. Cells were then washed three times with PBS, and secondary Ab was applied for 1 h at room temperature. Cells were washed, mounted in Vectashield (Vector Laboratories), and observed with a Zeiss LSM700 microscope (Leica, Wetzlar, Germany).

Duolink® Proximity Ligation in Situ Assay—Cells (4×10^4) were grown on chamber slides in the presence or absence of control siRNA or ERM-specific siRNA. After 48 h, medium was replaced by DMEM containing 0.1% BSA, and cells were stimulated or not with Bz-ATP. Fixation, permeabilization, and incubation with antibodies were performed according to the manufacturer's instructions for Duolink proximity ligation *in situ* assay. The anti-mouse P2X7R rabbit polyclonal Abs were used in association with anti-ezrin mouse mAb or with anti-calcineurin mouse mAb (negative control). The anti-ERM rabbit polyclonal Abs with anti-ezrin mouse mAb were used as a positive control. Fluorescent spots were counted, and the average numbers of spots per cell were calculated using Metamorph software (Universal Imaging Corp.). In the Duolink proximity ligation *in situ* assay, background spots detected with each single Ab were deducted from the numbers of spots found with two Abs specific for different proteins.

Calcium Experiments—Cells were transfected with control siRNA or ERM-specific siRNAs. After 48 h, cells were loaded with 2 μM Fura-2 AM (Molecular probes) in DMEM supplemented with 10% FCS (1 mM Ca^{2+}) for 30 min at 37 °C. Then cells were washed in modified Krebs-HEPES medium and suspended in this buffer. The modified Krebs-HEPES, pH 7.4 contained 128 mM NaCl, 2.5 mM KCl, 2.7 mM $CaCl_2$, 16 mM glucose, and 20 mM HEPES. We measured the increase in Ca^{2+} in cells by dual excitation spectrofluorometric analysis at 340 and 380 nm (ratio of A_{340}/A_{380}). Bz-ATP (300 μM) was added after 50 s, and Triton X-100 (0.1%) was added after 200 s.

Non-selective Pore Formation—Cells were transfected with control siRNA or ERM-specific siRNAs, seeded in a flat bottom 96-well plate, and cultured for 48 h. Cells were incubated in assay buffer containing 10 μg/ml ethidium bromide (EtBr) in DMEM containing 0.1% BSA. Bz-ATP (1 mM) was added, and fluorescence was monitored for 20 min at 37 °C in a spectrofluorometer (Wallac 1420) using an excitation wavelength of 485 nm and an emission wavelength of 615 nm.

Statistical Analysis—Data are expressed as means ± S.E. Data were analyzed using Student's *t* test, and $p < 0.05$ (*) (at least) was considered statistically significant. When data involved more than one variable, statistical significance was estimated with one-way ANOVA followed by Tukey's test using GraphPad software.

RESULTS

P2X7R Specifically Triggers ERM Phosphorylation—It has been shown previously that P2X7R stimulation induces the formation of blebs that are dependent on RhoA-dependent kinase activity (23, 42). Moreover, ERM control cell blebbing associated to some cellular processes (24). Thus, we investigated whether P2X7R stimulation modulates ERM phosphorylation. The levels of phospho-ERM proteins were measured in cell lysates of Neuro2a and Neuro2a-hAPP cells stimulated with 1 mM Bz-ATP, a selective agonist of P2X7R. Interestingly, Bz-ATP stimulation triggered ERM phosphorylation (Fig. 1*A*). The ratio of phospho-ERM *versus* total ezrin was increased 6-fold when Bz-ATP stimulated cells were compared with unstimulated cells (Fig. 1*A*, histograms). A kinetic study of Bz-ATP-induced ERM phosphorylation showed that phosphorylation increased rapidly, reached a maximum at 10–15 min, and decreased to the basal level at 30 min. These data show that Bz-ATP stimulation leads to ERM phosphorylation.

To establish that Bz-ATP induces ERM phosphorylation through P2X7R, we used as a first approach a selective pharmacological inhibitor of P2X7R (A438079). As shown in Fig. 1*A*, Bz-ATP stimulation of Neuro2a cells triggered ERM phosphorylation, whereas preincubation with a 10 μM concentration of the P2X7R inhibitor reduced it to basal levels. Furthermore, Bz-ATP-dependent ezrin and moesin phosphorylation was only observed in HEK cells expressing the mouse P2X7R and not in HEK control cells that did not express P2X7R (Fig. 1*B*). Finally, Bz-ATP stimulation induced ezrin and moesin phosphorylation in primary astrocytes of wild-type animals but not in astrocytes of P2X7R knock-out mice (Fig. 1*C*). In conclusion, these data demonstrate that Bz-ATP triggers ERM phosphorylation via P2X7R.

As human P2X7R has different pharmacological properties from mouse P2X7R, we determined whether P2X7R activation of human cells triggers ERM phosphorylation. Thus, we stimulated human neuroblastoma SK-N-BE cells with Bz-ATP. We found that P2X7R stimulation induces ERM phosphorylation specifically because it was inhibited by the P2X7R pharmacological inhibitor (Fig. 1*D*). Altogether, these results demonstrate that P2X7R stimulation leads to ERM phosphorylation in human and murine cells.

Bz-ATP Stimulation Triggers Ezrin Translocation to the Plasma Membrane—It has previously been established that ERM proteins undergo a major conformational change after phosphorylation and translocate to the plasma membrane (25, 26). Thus, we determined the consequences of P2X7R stimulation on the cellular distribution of ezrin. We stimulated Neuro2a cells expressing ezrin, its N-terminal domain fused to GFP, or GFP alone as a control with Bz-ATP. We followed the fate of GFP proteins by video microscopy. As shown in Fig. 2, 10 min after stimulation with Bz-ATP, ezrin-GFP had translocated to the plasma membrane (compare *C* and *D*), whereas GFP (control) remained cytoplasmic in both cases (Fig. 2, *A* and *B*). As described previously, the N-terminal ezrin-GFP was constitutively localized to the plasma membrane (41) and did not change with Bz-ATP (Fig. 2, *E* and *F*). These results indicate that P2X7R simulation leads to ezrin phosphorylation and to its

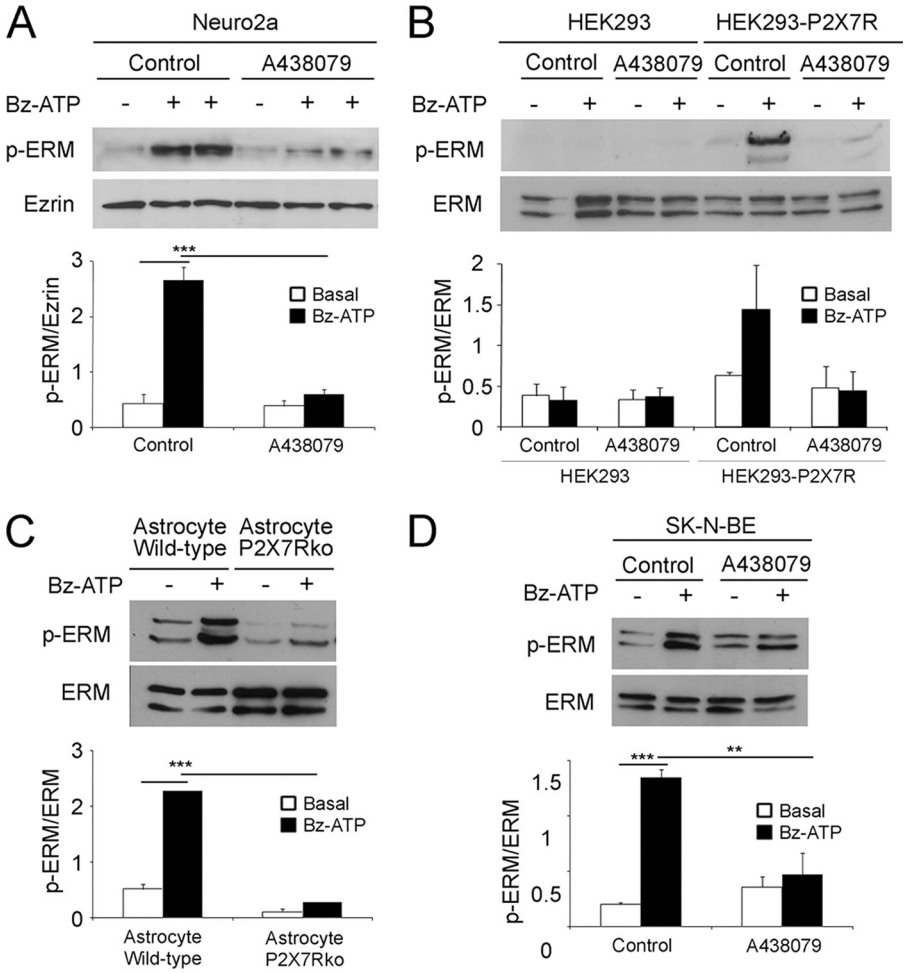

FIGURE 1. **ERM activation is specifically induced by P2X7R stimulation.** *A*, Neuro2a cells were pretreated with or without a pharmacological inhibitor of P2X7R (A438079) at 37 °C for 1 h and stimulated or not with 1 mM Bz-ATP for 10 min. Proteins from whole cell lysates of Neuro2a cells stimulated or not with 1 mM Bz-ATP were separated by SDS-PAGE. After transfer, the nitrocellulose membrane was probed with anti-phosphospecific ERM Abs (*upper panel*). The blot was stripped and probed with anti-ezrin Ab (*lower panel*). Blots were scanned, and the ratios of phosphorylated ERM (*p-ERM*) to total ezrin are presented as histograms. The graph shows the ratios of the phosphorylated ERM *versus* the total ezrin. Data are from four independent experiments (one-way ANOVA followed by Tukey's test, $F = 35.73$). *B*, HEK cells or mouse P2X7R stable transfectants of HEK cells were treated as in *A*. Cell lysates were analyzed by Western blot with anti-phosphospecific ERM (*upper* blot) or anti-ERM antibodies (*lower* blot). The graph shows the ratios of the phosphorylated ERM *versus* the total ERM. Data are from three independent experiments (one-way ANOVA followed by Tukey's test, $F = 4.18$). *C*, astrocytes from wild-type and P2X7R KO animals were treated or not with 1 mM Bz-ATP at 37 °C for 10 min. Whole cell lysates were analyzed by Western blot with anti-phosphospecific ERM Abs (*upper* blot) and by anti-ERM Abs (*lower* blot). Blots were scanned, and the ratios of phosphorylated ERM *versus* the total ERM are shown as histograms. Data are from three independent experiments (one-way ANOVA followed by Tukey's test, $F = 33.95$). *D*, the human neuroblastoma SK-N-BE cells were pretreated with or without A438079 at 37 °C for 1 h and stimulated with or without 1 mM Bz-ATP for 10 min. Whole cell lysates were prepared and analyzed by Western blot using anti-phosphospecific ERM (*upper* blot) or anti-ERM Abs (*lower* blot). Blots were scanned, and the ratios of phosphorylated ERM *versus* the total ERM are shown as histograms. Data are from three independent experiments (one-way ANOVA followed by Tukey's test, $F = 23.73$; *, $p < 0.05$; **, $p < 0.01$; ***, $p < 0.001$). *Error bars* represent S.E.

translocation to the plasma membrane. To determine whether P2X7R stimulation leads to translocation of phosphorylated ERM in untransfected cells, we labeled the plasma membrane of Neuro2a cells with DiI, and then these cells were stimulated or not with Bz-ATP and fixed with paraformaldehyde. After permeabilization, cells were labeled with anti-phospho-ERM Abs and analyzed. As shown in Fig. 2, phospho-ERM (*green* labeling) was localized at the plasma membrane (labeled in *red*; *H*), whereas no fluorescence was detected in unstimulated Neuro2a cells (*G*). These experiments establish that Bz-ATP stimulation triggers phosphorylation of ERM and their accumulation under the plasma membrane.

P2X7R Associates with Ezrin—We therefore investigated whether ezrin is capable to associate with P2X7R and whether this interaction is phosphodependent. Thus, the interaction between ezrin and P2X7R was assessed using the Duolink proximity ligation assay. This method relies on the use of two primary antibodies from two different species reacting with ezrin or P2X7R. A pair of oligonucleotide-labeled secondary antibodies is used to detect the bound primary antibodies. If the two different epitopes detected by these antibodies are close enough, the free oligonucleotide extremities are ligated by a DNA ligase, and an amplification reaction is triggered. The amplified products are then visualized with fluorescently labeled oligonucleotides (43). As shown in Fig. 3, each fluorescent spot is produced when the two oligonucleotide-labeled secondary antibodies are in close vicinity. Thus, the number of fluorescent spots/cell indicates that the epitopes detected by the primary antibodies are in close proximity (<25 nm). After P2X7R stimulation, the number of spots/cell increased 5-fold as

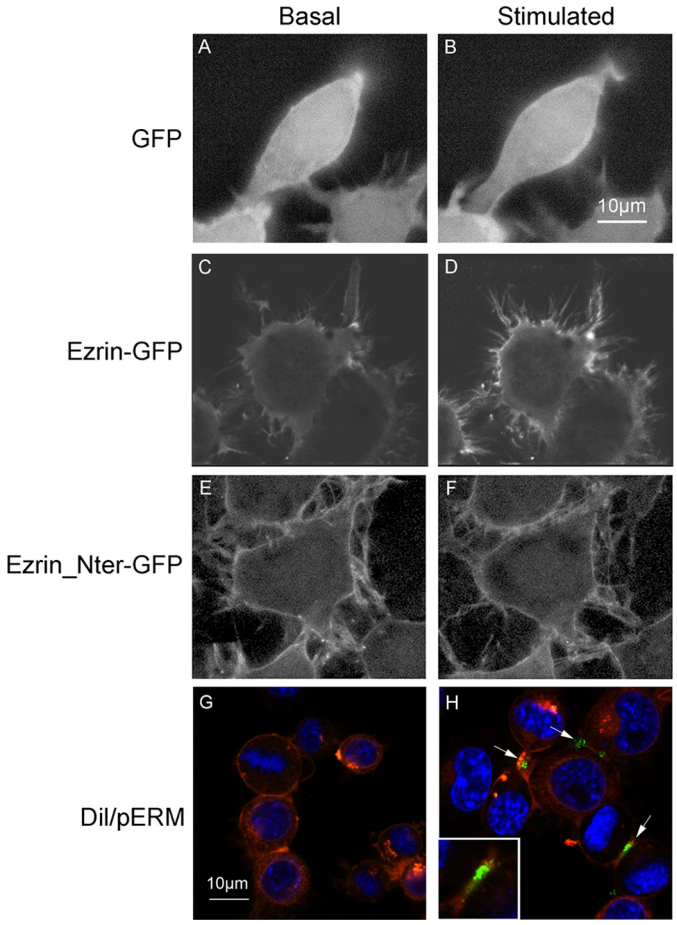

FIGURE 2. **Bz-ATP stimulation induces ezrin translocation to the plasma membrane.** Neuro2a cells were transfected with plasmids expressing GFP (*A* and *B*) or ezrin-GFP (*C* and *D*) or N-terminal domain (*Nter*) of ezrin-GFP (*E* and *F*). Cells were incubated at 37 °C in DMEM and treated with 1 mM Bz-ATP. GFP distribution was assessed by video microscopy. Pictures were taken before addition of Bz-ATP (*A*, *C*, and *E*) and 10 min after stimulation (*B*, *D*, and *F*). Neuro2a-hAPP cells, plated in a polylysine-coated Lab-Tek slide at 2×10^4 cells/well, were incubated with Dil cell labeling solution for 15 min and stimulated (*H*) or not (*G*) with Bz-ATP (1 mM) for 10 min. Fixed and permeabilized cells were labeled with rabbit anti-phosphospecific ERM Abs and then with Alexa Fluor 488-conjugated goat anti-rabbit IgG (*G* and *H*). *Arrows* show *green* fluorescence corresponding to phosphospecific ERM (*pERM*). The *inset* shows a 2× amplification of the image indicated by the *arrow* in the *right lower quadrant*. The results are representative of four experiments performed on different days.

compared with resting conditions, indicating that P2X7R and ezrin interact (Fig. 3, *A* and *B*). As expected, no interaction was detected between P2X7R and calcineurin (Fig. 3, *A* and *B*).

As shown in Fig. 3, *C* and *D*, the inhibition of ERM expression by ERM-specific siRNAs (Fig. 4*A*) led to a significant decrease in the number of spots/cell, which corresponds to the detection of ERM/ezrin epitopes. Importantly, as shown in Fig. 3, *E* and *F*, the number of fluorescent spots/cell representing P2X7R/ezrin interactions was reduced to background levels when cells were transfected with ERM-specific siRNA, whereas it was not with siRNA control.

ERM Are Not Required for P2X7R-dependent Cation Channel and Non-selective Pore Opening—The activation of P2X7R by extracellular ATP rapidly induces the opening of the cation channel and non-selective pore. Because P2X7R stimulation leads to ERM phosphorylation and increases P2X7R interaction with phospho-ERM, we determined whether ERM are involved in the opening of the cation channel and non-selective pore. As shown in Fig. 4, *B* and *C*, ERM-specific siRNAs did not affect the formations of cation channel, whereas non-selective pore formation was inhibited mildly (24.2 ± 1.6%) even though ERM expression was strongly inhibited (87 ± 4%) (Fig. 4, *A* and *E*). To determine whether the mild decrease in non-selective pore formation is due to a diminution of P2X7R in ERM-deficient cells, we compared the levels of P2X7R in Neuro2a cells transfected with control or ERM-specific siRNAs. As shown in Fig. 4*E*, the amounts of P2X7R were identical in both cell lysates.

ERM Activation Is Required for P2X7R-dependent sAPPα Shedding—We have shown previously that the stimulation of P2X7R triggers the proteolytic cleavage of APP and the release of sAPPα (4). Because we established that P2X7R activation leads to ERM phosphorylation in human and mouse tumor cell lines as well as in primary mouse astrocytes, we determined whether ERM proteins are involved in P2X7R-dependent sAPPα release. To this end, we used siRNAs of ezrin, radixin, and moesin to evaluate their impact on P2X7R-dependent shedding of sAPPα. First, we transfected Neuro2a cells with siRNAs to knock down the three proteins. As shown in Fig. 5*A* (*middle panel*), ezrin, radixin, and moesin expression was inhibited by siRNAs efficiently. In addition, Bz-ATP stimulation induced a strong phosphorylation of ERM in cells transfected with siRNA control, whereas very weak phosphorylated bands appeared in cells transfected with ERM-specific siRNAs (Fig. 5*A*, *upper* blot). We then evaluated the levels of sAPPα released in the supernatants of cells transfected with siRNAs and stimulated or not with Bz-ATP. The data clearly show that the amount of sAPPα released in the supernatant of cells transfected with ERM siRNAs was reduced (by 71.5 ± 5.8%) when compared with control (Fig. 5*B*). Thus, when ERM are knocked down, P2X7R stimulation is unable to trigger APP cleavage. However, one may argue that the expression level of APP is decreased when ERM are knocked out. Thus, we compared the amounts of APP present in Neuro2a cells transfected with control or ERM-specific siRNAs. Identical amounts of surface APP were found in lysates of Neuro2a cells transfected with both siRNAs (data not shown). Because plasma membrane APP represents only 10% of total APP (44), a decrease in cell surface APP might have escaped detection. Thus, we isolated biotinylated cell surface proteins by affinity chromatography with neutravidin beads and compared the amount of membrane APP expressed by Neuro2a cells transfected with siRNAs by Western blot. Our results clearly show that the levels of plasma membrane APP were identical in both cell samples, ruling out that a lack of ERM decreases APP expression and/or localization at the plasma membrane (Fig. 4*E* and data not shown).

The role of each ERM protein in the P2X7R-dependent cleavage of APP was determined using an siRNA specific for each. As observed in Fig. 5, *C*, *E*, and *G*, transfection with siRNA specific for ezrin, radixin, or moesin led to a strong and specific inhibition of the phosphorylated form of each protein. When ezrin and moesin were invalidated, sAPPα shedding was strongly inhibited (for ezrin, 69.7 ± 7.3%; for moesin, 77 ± 1.5%) after P2X7R activation (Fig. 5, *D* and *H*). In contrast, although there was an increased phosphorylation of radixin upon stimulation, a much weaker decrease in sAPPα release

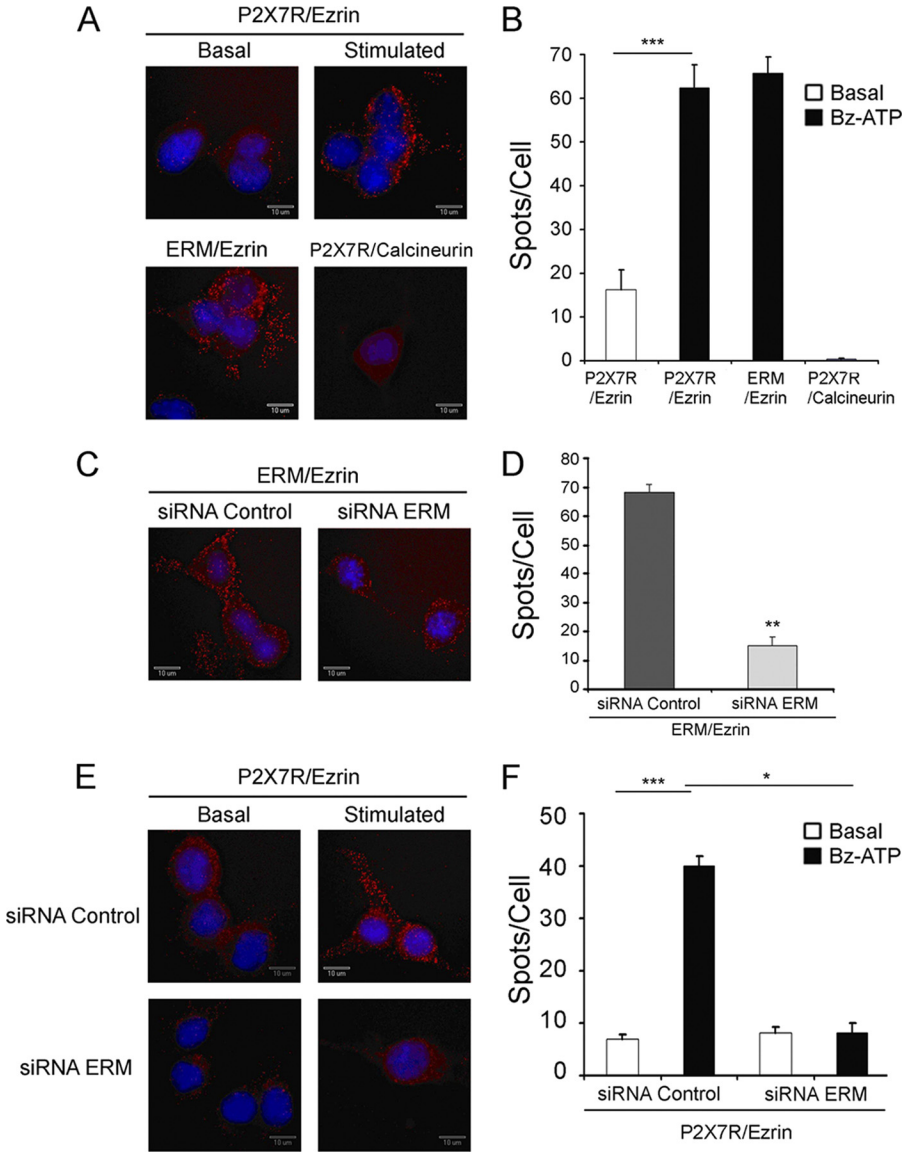

FIGURE 3. **Ezrin interacts with P2X7R.** Neuro2a cells were seeded on Lab-Tek slides and incubated for 48 h at 37 °C. *A*, cells were incubated without *Basal*) or with (*Stimulated*) 1 mM Bz-ATP for 10 min, fixed with 4% paraformaldehyde, permeabilized, and treated with rabbit anti-P2X7R Abs and mouse anti-ezrin mAb (*P2X7R/Ezrin*), with rabbit anti-ERM Abs and mouse anti-ezrin mAb (*ERM/Ezrin*; positive control), or with rabbit anti-P2X7R Abs and mouse anti-calcineurin mAb (*P2X7R/Calcineurin*; negative control). *B*, histograms represent the average values of the number of spots/cell in different fields ±S.E. For each condition, 150–200 cells were analyzed, and one representative experiment of at least three is presented. *C* and *E*, cells were transfected with control or ERM-specific siRNAs for 48 h, then stimulated or not with Bz-ATP for 10 min, fixed with 4% paraformaldehyde, permeabilized, and treated with rabbit anti-ERM Abs and mouse anti-ezrin mAb (*C*) or with rabbit anti-P2X7R Abs and mouse anti-ezrin mAb (*E*). *D* and *F*, histograms represent the average values of the number of spots/cell in different fields ±S.E. For each condition, at least 30 cells were analyzed, and one representative experiment of at least three is presented. The potential interaction of the proteins stained with antibodies was determined using the Duolink technology with two Abs from different species specific for each protein. Each spot indicates that molecules are in close proximity (distance <25 nm). *B*, one-way ANOVA followed by Tukey's test, $F = 84$; *D*, Student's *t* test; **, $p < 0.01$; *F*, one-way ANOVA followed by Tukey's test, $F = 10.44$; *, $p < 0.05$; ***, $p < 0.001$. *Error bars* represent S.E.

was observed (36.3 ± 1.9%) when radixin expression was inhibited (Fig. 5*F*). These experiments clearly show that ERM activation is required for the triggering of the proteolytic pathway leading to sAPPα shedding.

ERM Activation Is Not Always Associated with the Induction of sAPPα Shedding—To determine whether any stimulus leading to ERM phosphorylation triggers sAPPα release, we stimulated Neuro2a-hAPP cells with NGF. It is well established that NGF stimulates Neuro2a cells (45) and induces a rapid phosphorylation of ERM (46, 47). Thus, we treated Neuro2a cells with NGF and quantified the ratio of phospho-ERM/ERK (Fig. 6*B*) as well as the percentage of sAPPα released in the supernatants (Fig. 6*C*). The results clearly show that both NGF and Bz-ATP triggered ERM phosphorylation, but Bz-ATP stimulation only led to sAPPα shedding.

Biochemical Pathways Involved in the P2X7R-dependent Proteolytic Processing of APP—It has been established that P2X7R stimulation triggers Rho kinases (23). Thus, we determined whether fasudil, a pharmacological inhibitor of Rho kinase, blocks ERM phosphorylation and sAPPα shedding induced by P2X7R stimulation. As shown in Fig. 7, fasudil efficiently inhibited P2X7R-dependent ERM phosphorylation (Fig. 7*B*) and reduced the shedding of sAPPα to 58.8 ± 1.8% (Fig. 7*A*). Recently, we have demonstrated that the MAPK modules are

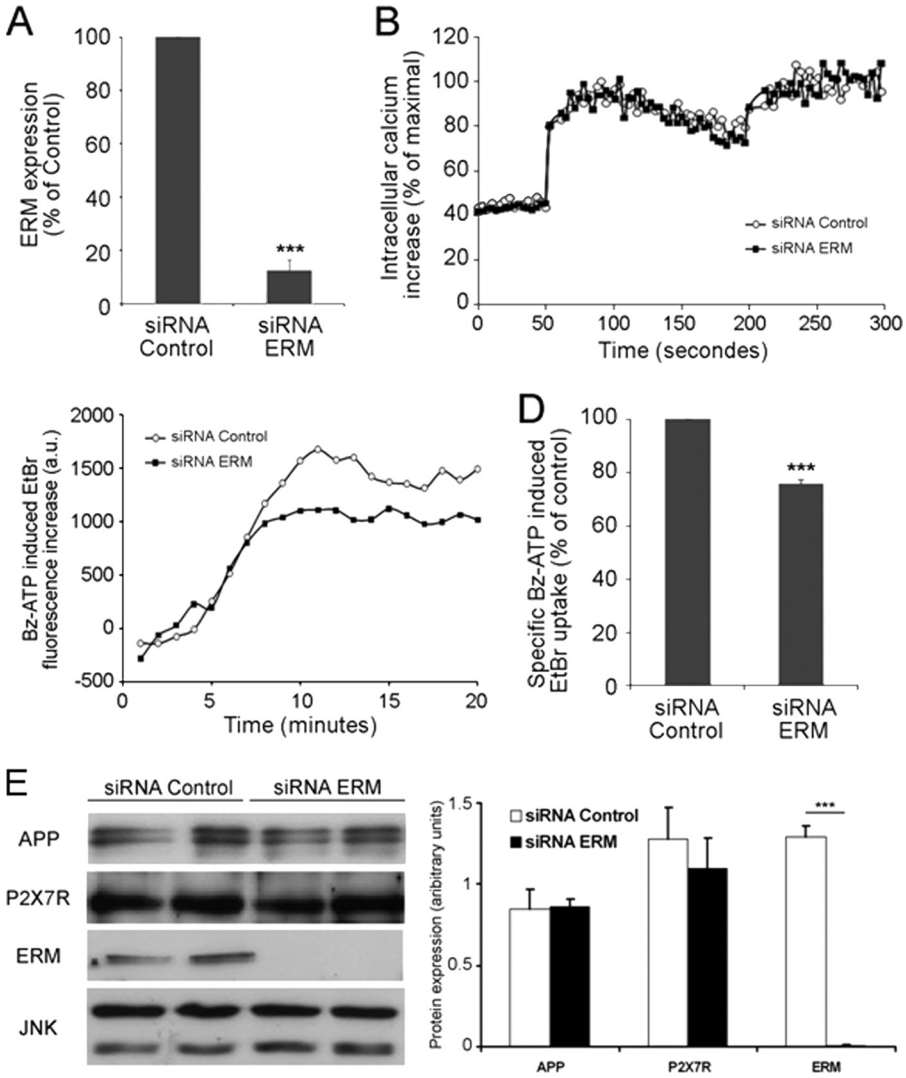

FIGURE 4. **P2X7R-dependent cation channel opening and non-selective pore formation are not or are mildly modulated by ERM, respectively.** *A*, Neuro2a cells were transfected with 3 μM control or ERM-specific siRNAs. After 48 h, cells were lysed, and proteins from cell lysates were analyzed by Western blot with anti-ERM Abs. The amounts of ERM in lysates from cells transfected with control siRNA or ERM-specific siRNAs were quantified. The percentage of inhibition of ERM proteins by specific siRNAs was calculated (Student's *t* test; ***, $p < 0.001$). *B*, Neuro2a cells were loaded with 2 μM Fura-2 AM 48 h after transfection with 3 μM control or ERM siRNAs, cells were stimulated with 300 μM Bz-ATP in modified Krebs-HEPES at 37 °C, and the maximal increase was obtained after addition of 0.1% Triton X-100. The Ca^{2+} increase was determined as described under "Experimental Procedures." *C*, Neuro2a cells were transfected with 3 μM control or ERM-specific siRNAs. After 48 h, cells were incubated with EtBr and stimulated with 1 mM Bz-ATP for increasing lengths of time. EtBr fluorescence of each sample was monitored for 20 min at 37 °C. For each curve, Bz-ATP-dependent EtBr uptake was calculated by subtracting EtBr values of unstimulated cells from values of Bz-ATP-stimulated cells. The results are representative of five experiments performed on different days. *a.u.*, arbitrary units. *D*, the graph shows the percentages of fluorescence obtained after stimulation with Bz-ATP of Neuro2a cells transfected with control or ERM siRNAs. The means of five EtBr fluorescence values at the plateau (from 15 to 20 min) were calculated for control siRNA- and ERM siRNA-transfected cells. The control siRNA values correspond to a 100% fluorescence increase. The percentage of fluorescence obtained in cells transfected with ERM siRNAs was calculated considering fluorescence of control siRNA-transfected cells as 100% (Student's *t* test; ***, $p < 0.001$). *E*, comparison of the amounts of APP and P2X7R present in lysates of Neuro2a cells transfected with control or ERM-specific siRNAs. Neuro2a cells were transfected with 3 μM control or ERM-specific siRNAs. After 48 h, cells were lysed, and proteins from cell lysates were analyzed in duplicate by Western blot with anti-APP, anti-P2X7R, anti-ERM, and anti-JNK Abs. The amounts of each protein were quantified. A comparison of the ratios of the protein levels *versus* JNK in lysates of cells transfected with control or ERM-specific siRNAs is shown in the *right panel*. A significant statistical difference was observed for ERM only (Student's *t* test; ***, $p < 0.001$). *Error bars* represent S.E.

activated after P2X7R stimulation (4). Moreover, the inhibition of the MAP kinases ERK1/2 and JNK but not p38 blocks P2X7R-dependent sAPPα shedding (4). To determine whether these MAPK modules are involved in ERM activation, we assessed the effect of specific pharmacological inhibitors of ERK and JNK on P2X7R-induced ERM activation in Neuro2a cells. We found that both inhibitors blocked ERM phosphorylation (Fig. 7*C*). These experiments demonstrate that the MAP kinases ERK1/2 and JNK are involved in ERM activation. Furthermore, using ERM-specific siRNA, we showed that the inhibition of ERM expression did not block MAP kinase ERK1/2 and JNK phosphorylation (Fig. 7*D*). Altogether, these experiments demonstrate that these Ser/Thr kinases are activated upstream of ERM proteins.

It has been shown previously that P2X7R stimulation of rat astrocytes and mouse thymocytes leads to phosphoinositide 3-kinase (PI3K) activation (8, 48). Furthermore, ezrin has been shown to interact with p85, the regulatory subunit of PI3K (29). Thus, we determined whether PI3K is involved in APP processing and ERM activation. LY294002 (10 μM) and wortmannin

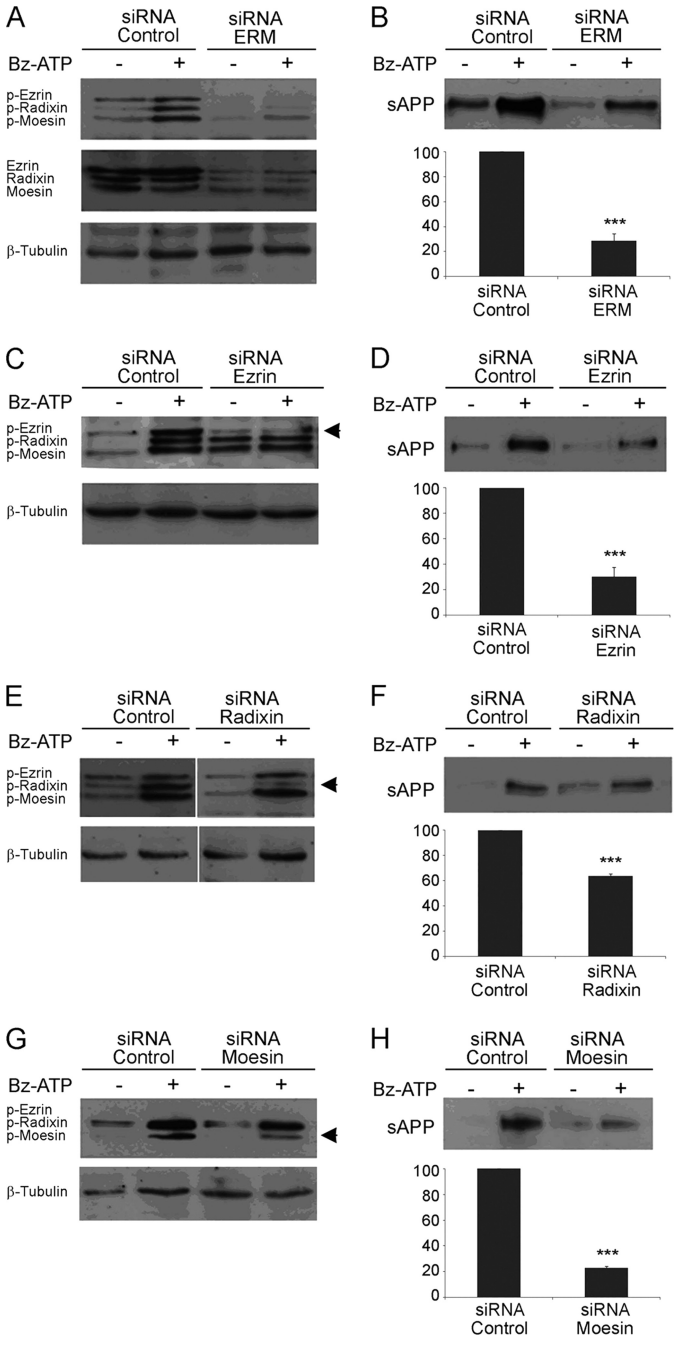

FIGURE 5. **ERM are involved in P2X7R-dependent sAPPα shedding.** *A*, Neuro2a cells were transfected with 3 μM control or ERM siRNAs. After 48 h, cells were stimulated or not with 1 mM Bz-ATP for 10 min. Proteins from cell lysates were analyzed by Western blot with anti-phosphospecific ERM (*A*, *upper* blot) or anti-ERM Abs (*A*, *middle* blot). After stripping, blots were probed with anti-β-tubulin mAb to show equal loading (*A*, *lower* blot). *B*, the supernatants of Neuro2a cells were analyzed for sAPPα shedding by Western blot. The amount of sAPPα released was quantified by densitometric analysis. The amount of sAPPα shed by Neuro2a cells stimulated with Bz-ATP minus the amount of spontaneous sAPPα release corresponds to the maximal amount of sAPPα shed. After siRNA knock-out of ERM, the percentage of sAPPα released corresponds to the quantity of sAPPα shed by stimulated cells minus the amount of spontaneous sAPPα released divided by the maximal amount of sAPPα shed in control conditions. Data are from five independent experiments (Student's *t* test; ***, $p < 0.001$). *C*, *E*, and *G*, Neuro2a cells were transfected by control or ezrin- (*C*), radixin- (*E*), or moesin (*G*)-specific siRNAs. After 48 h, the cells were stimulated or not with 1 mM Bz-ATP. The proteins from cell lysates were analyzed by Western blot using anti-phospho (*p*)-ERM Abs and after stripping with anti-β-tubulin mAb to control for equal loading. *D*, *F*, and *H*, the supernatants from Neuro2a cells described in *C*, *E*, and *G* were analyzed by Western blot to detect the amount of sAPPα released. After siRNA knock-out of each protein, the percentage of sAPPα released, which corresponds to the quantity of sAPPα shed by stimulated cells minus the amount of spontaneous sAPPα divided by the maximal amount of sAPPα shed in control conditions, was calculated. Data are from at least three independent experiments (Student's *t* test; ***, $p < 0.001$). *Error bars* represent S.E.

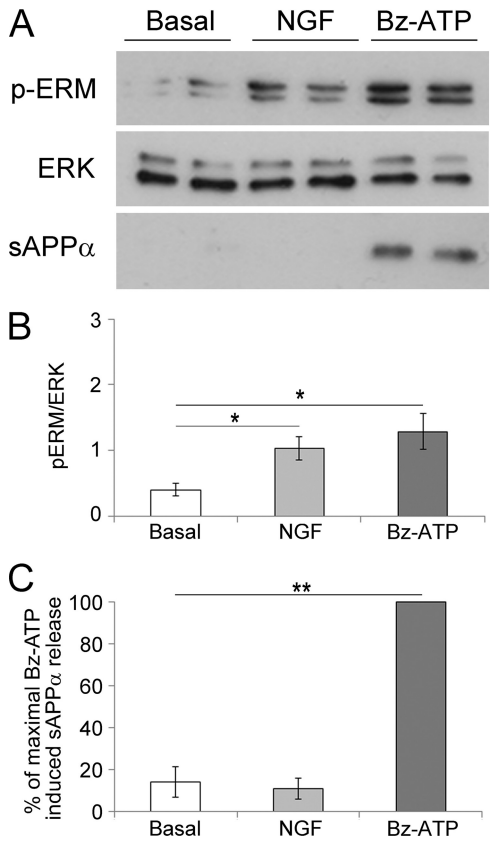

FIGURE 6. **NGF stimulation induces ERM phosphorylation but not sAPPα release.** *A*, Neuro2a cells were stimulated or not with 100 ng/ml NGF or 1 mM Bz-ATP for 15 min. Proteins from whole cell lysates of Neuro2a cells were separated by SDS-PAGE. After transfer, the nitrocellulose membrane was probed with anti-phosphospecific ERM Abs (*upper panel*). The blot was stripped and probed with anti-ERK Abs (*middle panel*). The supernatants of Neuro2a cells were analyzed for sAPPα shedding by Western blot (*lower panel*). *B*, blots were scanned, and the ratios of phosphorylated ERM by ERK are presented as histograms. The graph shows the ratios of the phosphorylated ERM (*pERM*) *versus* ERK. Data are from four independent experiments (Student's *t* test; *, $p < 0.05$). *C*, the amount of sAPPα released was quantified by densitometric analysis. The percentage of sAPPα shed by Neuro2a cells stimulated or not with NGF or Bz-ATP corresponds to the quantity of sAPPα shed divided by the amount of sAPPα released by Bz-ATP-stimulated cells $\times$ 100. Data are from three independent experiments (Student's *t* test; **, $p < 0.01$). *Error bars* represent S.E.

(50 μM), two pharmacological inhibitors of PI3K, strongly decreased sAPP shedding but did not block ERM phosphorylation on threonine (Fig. 7, *E* and *F*). Thus, PI3K is involved in the proteolytic cleavage of APP but acts downstream of ERM activation.

DISCUSSION

In this report, we demonstrate for the first time that ERM protein phosphorylation at Thr-567 and translocation to the membrane is required for the P2X7R-dependent proteolytic processing of APP leading to the shedding of sAPPα. Indeed, we have established that P2X7R stimulation triggers the phosphor-

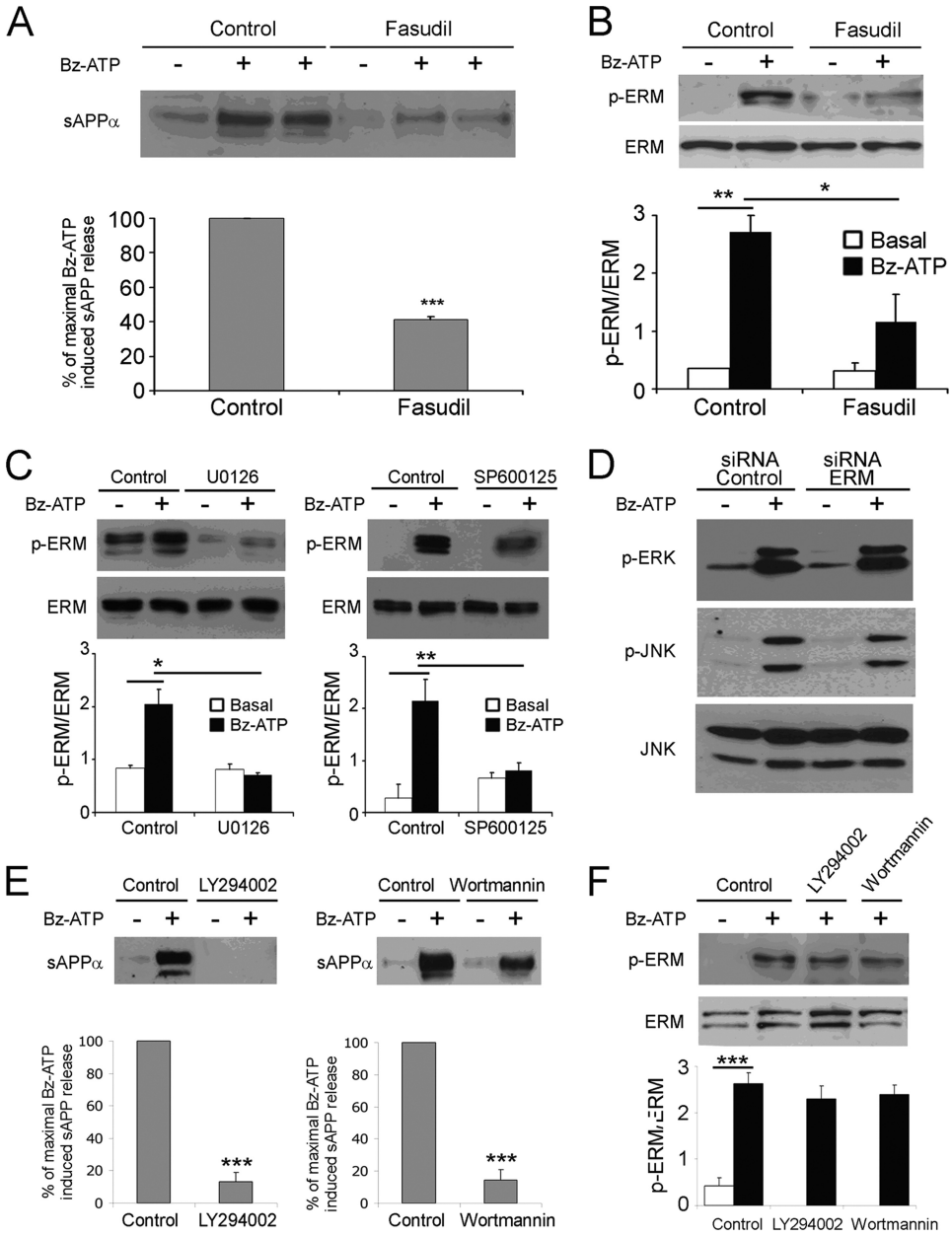

FIGURE 7. **P2X7R-dependent biochemical pathways involved in ERM activation.** *A* and *B*, Neuro2a cells were pretreated with or without 500 nM fasudil, a pharmacological inhibitor of Rho kinases, at 37 °C for 1 h and stimulated with 1 mM Bz-ATP for 10 min. *A*, the supernatants of Neuro2a cells were analyzed for sAPPα shedding by Western blot. Histograms correspond to densitometric analyses of sAPPα release as described under "Experimental Procedures." Values are the means ± S.E. of three independent experiments (Student's *t* test; ***, $p < 0.001$). *B*, cell lysates were analyzed by Western blot with anti-phosphospecific ERM Abs, and then the membrane was stripped and probed with anti-ERM Abs. Blots were scanned, and the ratios of phospho-ERM (*p-ERM*) *versus* total ERM are presented as histograms. Data are from at least three independent experiments (one-way ANOVA followed by Tukey's test, $F = 10.70$; *, $p < 0.05$; **, $p < 0.01$). *C*, Neuro2a cells were pretreated or not with 20 μM SP600125, an inhibitor of the MAP kinase JNK; with U0126, an inhibitor of MEK1/2; or with U0124, a negative control for U0126, at 37 °C for 1 h and stimulated with or without 1 mM Bz-ATP for 10 min. Lysates of Neuro2a cells were analyzed by Western blot to detect phospho-ERM (*upper panels*). After stripping, the blots were probed with anti-ERM Abs to show equal loading (*bottom panels*). Histograms represent the amount of phosphorylated ERM *versus* total ERM quantified by densitometric analysis. Data are from at least three independent experiments (one-way ANOVA followed by Tukey's test; for U0126, $F = 12.44$; for SP600125, $F = 9.13$). *D*, Neuro2a cells were transfected with control or ERM-specific siRNAs. After 48 h, cells were stimulated or not with 1 mM Bz-ATP for 10 min. Cell lysates were analyzed by Western blot with anti-phospho-ERK1/2 (Thr(P)-202/Tyr(P)-204) Abs (*D*, *upper* blot) or with anti-phospho-JNK1/2 (Thr(P)-183/Tyr(P)-185) Abs (*D*, *middle* blot). After stripping, the blot was probed with anti-total JNK1/2 Abs (*F*, lower blot). One representative experiment of at least three is presented. *E*, Neuro2a cells were preincubated at 37 °C with or without 50 μM wortmannin or 10 μM LY294002 for 1 h. Cells were stimulated with 1 mM Bz-ATP at 37 °C for 10 min. Supernatants were analyzed by Western blot to quantify sAPPα. Histograms show the percentages of maximal sAPP release. Data are from three independent experiments (Student's *t* test; ***, $p < 0.001$). In *F*, cell lysates were analyzed to detect phosphorylated ERM (*upper panel*) and total ERM (*lower panel*). The graph shows the ratios of the phosphorylated ERM *versus* the total ERM. Data are from three independent experiments (one-way ANOVA followed by Tukey's test, $F = 23.53$). *Error bars* represent S.E.

ylation of ERM, which translocate to the plasma membrane where they associate with P2X7R. We have shown that the down-regulation of ERM by siRNA blocks the P2X7R-dependent shedding of sAPPα. In addition, using pharmacological inhibitors, we have been able to determine that a Rho kinase and the MAPK modules ERK1/2 and JNK are upstream of ERM proteins, whereas PI3K activity is downstream. Several groups have shown that P2X7R stimulation induces the formation of blebs that are dependent on RhoA-dependent kinase activity (23, 42). Because bleb formation involves ERM proteins (49), we investigated whether P2X7R stimulation induces ERM phosphorylation and determined the consequences of ERM activation. We found that P2X7R stimulation triggered the phosphorylation of a C-terminal threonine in ERM proteins and the shedding of sAPPα. Several candidate ERM kinases have been proposed among which PKC-θ (50), Rho kinase (51), Slik (37), and more recently lymphocyte-oriented kinase in lymphocytes (52). In our studies, we found that the Rho kinase inhibitor fasudil (Fig. 7, *A* and *B*) inhibited ERM phosphorylation and the release of sAPPα following P2X7R stimulation. These results are in agreement with two reports that indicate that P2X7R triggers Rho-A and Rho-A kinase activity in HEK-P2X7R cells, macrophages, and microglial cells (42, 53).

Because ERM phosphorylation is required for the shedding of sAPPα, one can hypothesize that any stimulus triggering ERM phosphorylation should lead to the proteolytic processing of APP and sAPPα release. Thus, we stimulated Neuro2a cells with NGF and showed that this stimulus induced ERM activation without sAPPα production. These results suggest that following ERM phosphorylation the biochemical pathways diverge. Indeed, in most cellular models, P2X7R stimulation leads to cell death, whereas NGF triggers cell growth and survival.

Crystallographic studies have shown that ERM are composed of an N-terminal FERM domain, an α-helical domain, and a C-terminal region that binds F-actin (54). The FERM domain directly interacts with phosphatidylinositol 4,5-bisphosphate and the cytoplasmic regions of transmembrane glycoproteins such as CD43; CD44; ICAM1, -2, and -3; and the neutral endopeptidase 24.11 (55–60). In addition, the FERM domain binds to the adaptor proteins sodium-hydrogen exchanger regulatory factors NHERF-1 and NHERF-2, also called ERM-binding phosphoprotein of 50 kDa (for a review, see Ref.61). These adaptor proteins interact by their C-terminal domain with ERM and by their PDZ1 domain with C-terminal motifs of several G-protein-coupled receptors and receptor tyrosine kinases (61). Thus, NHERF proteins play a major role in controlling the trafficking and turnover of several membrane receptors and in recruiting enzymes implicated in signal transduction (61, 62).

We have established that P2X7R associates with ERM proteins. A direct interaction of P2X7R with ERM is likely according to our proximity ligation assay, but we cannot rule out that an undefined motif allows the binding to an adaptor protein. Two proteomics studies have identified several proteins associated to P2X7R in P2X7 transfected HEK293 cells (63, 64) and in interferon γ-differentiated human monocytic leukemic THP-1 cells (64). In these studies, ERM were not found among the proteins co-purifying with P2X7R probably because both proteomics analyzes were performed on resting cells and ERM become linked to P2X7R only after stimulation of the receptor.

Our studies have also shown that ERM are not involved in the early biochemical steps of P2X7R activation because cation channel opening was not affected by ERM knockdown, whereas non-selective pore formation was moderately inhibited. In addition, this decrease in pore formation cannot be attributed to a down-modulation of P2X7R because the amounts of P2X7R found in lysates of Neuro2a cells transfected with control siRNA or ERM siRNA were undistinguishable (Fig. 4*E*). Recently, Gu *et al.* (64) have shown that P2X7R is associated with non-muscle myosin II and that ATP triggers the dissociation of P2X7R from myosin II. In addition, decreased expression of myosin II by specific shRNA enhances the non-selective pore formation following P2X7R stimulation. Thus, proteins transiently associated with P2X7R can regulate the non-selective pore formation. Indeed, P2X7R dissociation from non-muscle myosin is required for pore opening, whereas binding of P2X7R to ERM may potentiate this phenomenon.

Activated ERM undergo additional phosphorylation on Tyr-353, which binds PI3K (29). This induces the phosphorylation of Akt/PKB, which phosphorylates several substrates involved in survival pathways. The activation of P2X7R stimulated PI3K activity that was located downstream of ERM (Fig. 7*F*). However, this activity did not trigger the phosphorylation of Akt/PKB in Bz-ATP-treated Neuro2a cells (data not shown), a result in agreement with our previous work on P2X7R-mediated thymocyte death in which PI3K activity does not trigger the pro-survival Akt/PKB pathway (8). Our present data strongly suggest that PI3K participates in the biochemical pathway leading to sAPPα release because wortmannin, a broad spectrum inhibitor of phosphatidylinositol kinases, and a specific PI3K inhibitor prevented the P2X7-dependent processing of APP (Fig. 7*E*). Pretreatment of Neuro2a cells with the PI3K inhibitors did not block ERM phosphorylation on threonine (Fig. 7*F*), indicating that P2X7R signaling in Neuro2a cells leads to ERM phosphorylation via activation of Rho kinase and MAP kinases, whereas PI3K is downstream of ERM. The involvement of PI3K in the shedding of sAPPα was also found when human neuroblastoma SH-SY5Y cells were stimulated with insulin-like growth factor-1 (65, 66). In this model, PI3K activity increased the level of ADAM10, which is involved in the non-amyloidogenic processing of APP (66). However, we have shown previously that the simultaneous silencing of ADAM9, -10, and -17 does not block the P2X7R-mediated proteolytic processing of APP, indicating that an unidentified α-secretase is also triggered by PI3K (4).

Our previous studies have shown that P2X7R stimulation induces a rapid activation of three MAP kinase modules, ERK1/2, JNK, and p38 (4). Importantly, using several pharmacological inhibitors, we have found that inhibition of MAP kinase ERK1/2 and JNK phosphorylation leads to a profound decrease in sAPPα release (4). In the present work, we have established a role, upstream of the ERM proteins, for the MAP kinase ERK1/2 and JNK modules in P2X7R-induced sAPPα shedding because pharmacological inhibition of MAP kinases blocked ERM phosphorylation (Fig. 7*C*), whereas ERM-specific

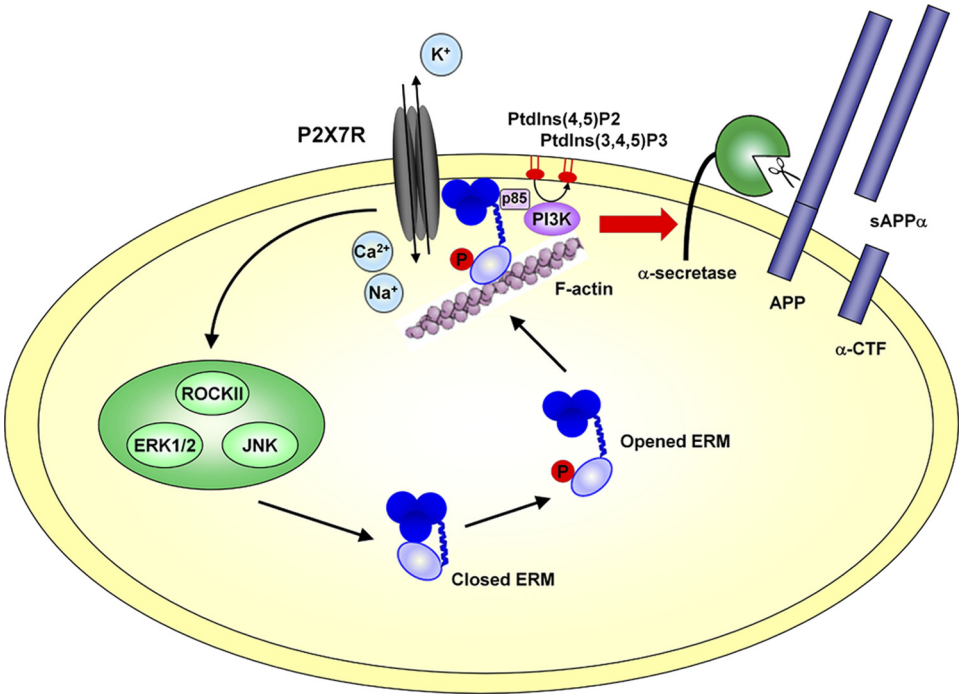

FIGURE 8. **Schematic representation of the biochemical pathways involved in P2X7R-dependent proteolytic cleavage of APP.** P2X7R stimulation by Bz-ATP triggers Ca^{2+} influx and activates the Rho kinase and the MAP kinases ERK1/2 and JNK. These Ser/Thr kinases directly or indirectly phosphorylate the ERM, which in turn translocate at the plasma membrane where they interact with P2X7R. The PI3K activity acts downstream of ERM. We hypothesize that its regulatory subunit is recruited through an SH2 domain to a phosphorylated tyrosine of ezrin as shown by Gautreau *et al.* (29). *PtdIns*, phosphatidylinositol; *ROCKII*, Rho kinase II; *CTF*, C-terminal fragment.

siRNAs did not abolish MAP kinase activation following P2X7R stimulation (Fig. 7*D*).

It is well established that the well known α-secretases ADAM9, -10, and -17 are able to cleave membrane APP to generate the non-amyloidogenic soluble fragment. Kommadi *et al.* (67) have demonstrated that phosphorylation at Thr-735 of ADAM17 is required for p75 neurotrophin receptor cleavage because ADAM17-deficient cells were reconstituted with wild-type ADAM17 but not with ADAM17 T735A mutant protease. In contrast, Le Gall *et al.* (68) have shown recently that the cytoplasmic domain of ADAM17 containing Thr-735 is not required for its activation by several physiological ligands. In addition, although there are Thr and Ser residues, which are potential phosphorylation sites, in the cytoplasmic tails of various ADAMs, to the best of our knowledge up to now, there is no indication that phosphorylation is required for ADAM activation other than ADAM17. In our previous work, we have demonstrated that the P2X7R-mediated sAPPα shedding is due to an unidentified TAPI2-GM6001-sensitive metalloprotease (4). At the present time, it is impossible to predict whether phosphorylation of this α-secretase is involved in its activation or trafficking.

APP can be phosphorylated at Thr-668 in its cytoplasmic region by several kinases such as cyclin-dependent kinase-5, glycogen synthase kinase-3β, and the MAP kinase JNK (69). The physiological role of APP phosphorylation at Thr-668 is controversial. Two studies have suggested it triggered β-secretase processing leading to amyloid β production (70, 71), whereas Feyt *et al.* (72) have found that phosphorylation of APP decreases γ-secretase processing and amyloid β production. Presently, data from the scientific literature suggest that the main consequences of Thr-668 phosphorylation come from a conformational modification that affects APP interactions with adaptor and scaffolding proteins such as Fe65, X11, and JNK-interacting protein 1b (for reviews, see Refs. 69 and 73). In our experimental model, JNK activity is required for ERM activation because pharmacological inhibition of JNK blocked ERM phosphorylation and sAPP shedding (Fig. 7*C*). Thus, in the P2X7R pathway, JNK probably phosphorylates ERM directly or via an undefined kinase, although we cannot rule out that JNK phosphorylates APP as well. ERK1/2 are also needed for ERM activation, so both ERK1/2 and JNK may phosphorylate concomitantly an unidentified kinase specific for the ERM. Alternatively, the two MAP kinases could act sequentially, one of them activating the ERM.

The present study establishes that ERM phosphorylation is required for the P2X7R-dependent non-amyloidogenic processing of APP. Furthermore, using siRNA and pharmacological inhibitors, we have identified the biochemical pathways leading to sAPPα shedding. We have shown that RhoA kinase and the MAP kinases ERK1/2 and JNK are upstream of ERM, whereas PI3K is located downstream (Fig. 8). Thus, complex interactions between transmembrane receptors, ERM, and F-actin may trigger the activation and the possible relocalization of α-secretases as has been observed with G-protein-coupled receptors (74, 75). We hypothesize that ERM are key components in the non-amyloidogenic pathway because they drive the clustering of transmembrane α-secretases with their substrates such as APP.

Acknowledgment—We thank Dr. Sylvain Le Gall for critical review of our manuscript.

REFERENCES

1. Gandy, S. (2005) The role of cerebral amyloid β accumulation in common forms of Alzheimer disease. *J. Clin. Investig.* **115,** 1121–1129
2. Wilquet, V., and De Strooper, B. (2004) Amyloid-β precursor protein processing in neurodegeneration. *Curr. Opin. Neurobiol.* **14,** 582–588
3. Mattson, M. P. (1997) Cellular actions of β-amyloid precursor protein and its soluble and fibrillogenic derivatives. *Physiol. Rev.* **77,** 1081–1132
4. Delarasse, C., Auger, R., Gonnord, P., Fontaine, B., and Kanellopoulos, J. M. (2011) The purinergic receptor P2X7 triggers α-secretase-dependent processing of the amyloid precursor protein. *J. Biol. Chem.* **286,** 2596–2606
5. Schachter, J., Motta, A. P., de Souza Zamorano, A., da Silva-Souza, H. A., Guimarães, M. Z., and Persechini, P. M. (2008) ATP-induced P2X7-associated uptake of large molecules involves distinct mechanisms for cations and anions in macrophages. *J. Cell Sci.* **121,** 3261–3270
6. Wilson, H. L., Wilson, S. A., Surprenant, A., and North, R. A. (2002) Epithelial membrane proteins induce membrane blebbing and interact with the P2X7 receptor C terminus. *J. Biol. Chem.* **277,** 34017–34023
7. Ferrari, D., Los, M., Bauer, M. K., Vandenabeele, P., Wesselborg, S., and Schulze-Osthoff, K. (1999) P2Z purinoreceptor ligation induces activation of caspases with distinct roles in apoptotic and necrotic alterations of cell death. *FEBS Lett.* **447,** 71–75
8. Auger, R., Motta, I., Benihoud, K., Ojcius, D. M., and Kanellopoulos, J. M. (2005) A role for mitogen-activated protein kinase (Erk1/2) activation and non-selective pore formation in P2X7 receptor-mediated thymocyte death. *J. Biol. Chem.* **280,** 28142–28151
9. Delarasse, C., Gonnord, P., Galante, M., Auger, R., Daniel, H., Motta, I., and Kanellopoulos, J. M. (2009) Neural progenitor cell death is induced by extracellular ATP via ligation of P2X7 receptor. *J. Neurochem.* **109,** 846–857
10. Adinolfi, E., Callegari, M. G., Cirillo, M., Pinton, P., Giorgi, C., Cavagna, D., Rizzuto, R., and Di Virgilio, F. (2009) Expression of the P2X7 receptor increases the Ca^{2+} content of the endoplasmic reticulum, activates NFATc1, and protects from apoptosis. *J. Biol. Chem.* **284,** 10120–10128
11. Adinolfi, E., Cirillo, M., Woltersdorf, R., Falzoni, S., Chiozzi, P., Pellegatti, P., Callegari, M. G., Sandonà, D., Markwardt, F., Schmalzing, G., and Di Virgilio, F. (2010) Trophic activity of a naturally occurring truncated isoform of the P2X7 receptor. *FASEB J.* **24,** 3393–3404
12. Colomar, A., Marty, V., Médina, C., Combe, C., Parnet, P., and Amédée, T. (2003) Maturation and release of interleukin-1β by lipopolysaccharide-primed mouse Schwann cells require the stimulation of P2X7 receptors. *J. Biol. Chem.* **278,** 30732–30740
13. Kahlenberg, J. M., and Dubyak, G. R. (2004) Mechanisms of caspase-1 activation by P2X7 receptor-mediated K^+ release. *Am. J. Physiol. Cell Physiol.* **286,** C1100–C1108
14. Solle, M., Labasi, J., Perregaux, D. G., Stam, E., Petrushova, N., Koller, B. H., Griffiths, R. J., and Gabel, C. A. (2001) Altered cytokine production in mice lacking $P2X_7$ receptors. *J. Biol. Chem.* **276,** 125–132
15. MacKenzie, A., Wilson, H. L., Kiss-Toth, E., Dower, S. K., North, R. A., and Surprenant, A. (2001) Rapid secretion of interleukin-1β by microvesicle shedding. *Immunity* **15,** 825–835
16. Lammas, D. A., Stober, C., Harvey, C. J., Kendrick, N., Panchalingam, S., and Kumararatne, D. S. (1997) ATP-induced killing of mycobacteria by human macrophages is mediated by purinergic P2Z(P2X7) receptors. *Immunity* **7,** 433–444
17. Coutinho-Silva, R., Stahl, L., Raymond, M. N., Jungas, T., Verbeke, P., Burnstock, G., Darville, T., and Ojcius, D. M. (2003) Inhibition of chlamydial infectious activity due to P2X7R-dependent phospholipase D activation. *Immunity* **19,** 403–412
18. Garbers, C., Jänner, N., Chalaris, A., Moss, M. L., Floss, D. M., Meyer, D., Koch-Nolte, F., Rose-John, S., and Scheller, J. (2011) Species specificity of ADAM10 and ADAM17 proteins in interleukin-6 (IL-6) trans-signaling and novel role of ADAM10 in inducible IL-6 receptor shedding. *J. Biol. Chem.* **286,** 14804–14811
19. Gu, B., Bendall, L. J., and Wiley, J. S. (1998) Adenosine triphosphate-induced shedding of CD23 and L-selectin (CD62L) from lymphocytes is mediated by the same receptor but different metalloproteases. *Blood* **92,** 946–951
20. Gu, B. J., and Wiley, J. S. (2006) Rapid ATP-induced release of matrix metalloproteinase 9 is mediated by the P2X7 receptor. *Blood* **107,** 4946–4953
21. Moon, H., Na, H. Y., Chong, K. H., and Kim, T. J. (2006) P2X7 receptor-dependent ATP-induced shedding of CD27 in mouse lymphocytes. *Immunol. Lett.* **102,** 98–105
22. Suzuki, T., Hide, I., Ido, K., Kohsaka, S., Inoue, K., and Nakata, Y. (2004) Production and release of neuroprotective tumor necrosis factor by P2X7 receptor-activated microglia. *J. Neurosci.* **24,** 1–7
23. Morelli, A., Chiozzi, P., Chiesa, A., Ferrari, D., Sanz, J. M., Falzoni, S., Pinton, P., Rizzuto, R., Olson, M. F., and Di Virgilio, F. (2003) Extracellular ATP causes ROCK I-dependent bleb formation in P2X7-transfected HEK293 cells. *Mol. Biol. Cell* **14,** 2655–2664
24. Roubinet, C., Decelle, B., Chicanne, G., Dorn, J. F., Payrastre, B., Payre, F., and Carreno, S. (2011) Molecular networks linked by Moesin drive remodeling of the cell cortex during mitosis. *J. Cell Biol.* **195,** 99–112
25. Charrin, S., and Alcover, A. (2006) Role of ERM (ezrin-radixin-moesin) proteins in T lymphocyte polarization, immune synapse formation and in T cell receptor-mediated signaling. *Front. Biosci.* **11,** 1987–1997
26. Fiévet, B., Louvard, D., and Arpin, M. (2007) ERM proteins in epithelial cell organization and functions. *Biochim. Biophys. Acta* **1773,** 653–660
27. Fehon, R. G., McClatchey, A. I., and Bretscher, A. (2010) Organizing the cell cortex: the role of ERM proteins. *Nat. Rev. Mol. Cell Biol.* **11,** 276–287
28. Arpin, M., Chirivino, D., Naba, A., and Zwaenepoel, I. (2011) Emerging role for ERM proteins in cell adhesion and migration. *Cell Adh. Migr.* **5,** 199–206
29. Gautreau, A., Poullet, P., Louvard, D., and Arpin, M. (1999) Ezrin, a plasma membrane-microfilament linker, signals cell survival through the phosphatidylinositol 3-kinase/Akt pathway. *Proc. Natl. Acad. Sci. U.S.A.* **96,** 7300–7305
30. Chirivino, D., Del Maestro, L., Formstecher, E., Hupé, P., Raposo, G., Louvard, D., and Arpin, M. (2011) The ERM proteins interact with the HOPS complex to regulate the maturation of endosomes. *Mol. Biol. Cell* **22,** 375–385
31. Poullet, P., Gautreau, A., Kadaré, G., Girault, J. A., Louvard, D., and Arpin, M. (2001) Ezrin interacts with focal adhesion kinase and induces its activation independently of cell-matrix adhesion. *J. Biol. Chem.* **276,** 37686–37691
32. Srivastava, J., Elliott, B. E., Louvard, D., and Arpin, M. (2005) Src-dependent ezrin phosphorylation in adhesion-mediated signaling. *Mol. Biol. Cell* **16,** 1481–1490
33. Pujuguet, P., Del Maestro, L., Gautreau, A., Louvard, D., and Arpin, M. (2003) Ezrin regulates E-cadherin-dependent adherens junction assembly through Rac1 activation. *Mol. Biol. Cell* **14,** 2181–2191
34. Darmellah, A., Rücker-Martin, C., and Feuvray, D. (2009) ERM proteins mediate the effects of Na^+/H^+ exchanger (NHE1) activation in cardiac myocytes. *Cardiovasc. Res.* **81,** 294–300
35. Killock, D. J., Parsons, M., Zarrouk, M., Ameer-Beg, S. M., Ridley, A. J., Haskard, D. O., Zvelebil, M., and Ivetic, A. (2009) *In vitro* and *in vivo* characterization of molecular interactions between calmodulin, ezrin/radixin/moesin, and L-selectin. *J. Biol. Chem.* **284,** 8833–8845
36. Yonemura, S., Tsukita, S., and Tsukita, S. (1999) Direct involvement of ezrin/radixin/moesin (ERM)-binding membrane proteins in the organization of microvilli in collaboration with activated ERM proteins. *J. Cell Biol.* **145,** 1497–1509
37. Carreno, S., Kouranti, I., Glusman, E. S., Fuller, M. T., Echard, A., and Payre, F. (2008) Moesin and its activating kinase Slik are required for cortical stability and microtubule organization in mitotic cells. *J. Cell Biol.* **180,** 739–746
38. Lasserre, R., Charrin, S., Cuche, C., Danckaert, A., Thoulouze, M. I., de Chaumont, F., Duong, T., Perrault, N., Varin-Blank, N., Olivo-Marin, J. C., Etienne-Manneville, S., Arpin, M., Di Bartolo, V., and Alcover, A. (2010) Ezrin tunes T-cell activation by controlling Dlg1 and microtubule positioning at the immunological synapse. *EMBO J.* **29,** 2301–2314
39. Niggli, V., and Rossy, J. (2008) Ezrin/radixin/moesin: versatile controllers of signaling molecules and of the cortical cytoskeleton. *Int. J. Biochem. Cell Biol.* **40,** 344–349

40. Yonemura, S., Hirao, M., Doi, Y., Takahashi, N., Kondo, T., Tsukita, S., and Tsukita, S. (1998) Ezrin/radixin/moesin (ERM) proteins bind to a positively charged amino acid cluster in the juxta-membrane cytoplasmic domain of CD44, CD43, and ICAM-2. *J. Cell Biol.* **140,** 885–895
41. Fievet, B. T., Gautreau, A., Roy, C., Del Maestro, L., Mangeat, P., Louvard, D., and Arpin, M. (2004) Phosphoinositide binding and phosphorylation act sequentially in the activation mechanism of ezrin. *J. Cell Biol.* **164,** 653–659
42. Verhoef, P. A., Estacion, M., Schilling, W., and Dubyak, G. R. (2003) P2X7 receptor-dependent blebbing and the activation of Rho-effector kinases, caspases, and IL-1β release. *J. Immunol.* **170,** 5728–5738
43. Fredriksson, S., Gullberg, M., Jarvius, J., Olsson, C., Pietras, K., Gústafsdóttir, S. M., Ostman, A., and Landegren, U. (2002) Protein detection using proximity-dependent DNA ligation assays. *Nat. Biotechnol.* **20,** 473–477
44. Thinakaran, G., and Koo, E. H. (2008) Amyloid precursor protein trafficking, processing, and function. *J. Biol. Chem.* **283,** 29615–29619
45. Pastor, R., Bernal, J., and Rodríguez-Peña, A. (1994) Unliganded c-erbA/thyroid hormone receptor induces trkB expression in neuroblastoma cells. *Oncogene* **9,** 1081–1089
46. Jeon, S., Park, J. K., Bae, C. D., and Park, J. (2010) NGF-induced moesin phosphorylation is mediated by the PI3K, Rac1 and Akt and required for neurite formation in PC12 cells. *Neurochem. Int.* **56,** 810–818
47. Marsick, B. M., San Miguel-Ruiz, J. E., and Letourneau, P. C. (2012) Activation of ezrin/radixin/moesin mediates attractive growth cone guidance through regulation of growth cone actin and adhesion receptors. *J. Neurosci.* **32,** 282–296
48. Jacques-Silva, M. C., Rodnight, R., Lenz, G., Liao, Z., Kong, Q., Tran, M., Kang, Y., Gonzalez, F. A., Weisman, G. A., and Neary, J. T. (2004) P2X7 receptors stimulate AKT phosphorylation in astrocytes. *Br. J. Pharmacol.* **141,** 1106–1117
49. Charras, G. T. (2008) A short history of blebbing. *J. Microsc.* **231,** 466–478
50. Pietromonaco, S. F., Simons, P. C., Altman, A., and Elias, L. (1998) Protein kinase C-theta phosphorylation of moesin in the actin-binding sequence. *J. Biol. Chem.* **273,** 7594–7603
51. Matsui, T., Maeda, M., Doi, Y., Yonemura, S., Amano, M., Kaibuchi, K., Tsukita, S., and Tsukita, S. (1998) Rho-kinase phosphorylates COOH-terminal threonines of ezrin/radixin/moesin (ERM) proteins and regulates their head-to-tail association. *J. Cell Biol.* **140,** 647–657
52. Belkina, N. V., Liu, Y., Hao, J. J., Karasuyama, H., and Shaw, S. (2009) LOK is a major ERM kinase in resting lymphocytes and regulates cytoskeletal rearrangement through ERM phosphorylation. *Proc. Natl. Acad. Sci. U.S.A.* **106,** 4707–4712
53. Takenouchi, T., Iwamaru, Y., Sugama, S., Sato, M., Hashimoto, M., and Kitani, H. (2008) Lysophospholipids and ATP mutually suppress maturation and release of IL-1β in mouse microglial cells using a Rho-dependent pathway. *J. Immunol.* **180,** 7827–7839
54. Li, Q., Nance, M. R., Kulikauskas, R., Nyberg, K., Fehon, R., Karplus, P. A., Bretscher, A., and Tesmer, J. J. (2007) Self-masking in an intact ERM-merlin protein: an active role for the central α-helical domain. *J. Mol. Biol.* **365,** 1446–1459
55. Alonso-Lebrero, J. L., Serrador, J. M., Domínguez-Jiménez, C., Barreiro, O., Luque, A., del Pozo, M. A., Snapp, K., Kansas, G., Schwartz-Albiez, R., Furthmayr, H., Lozano, F., and Sánchez-Madrid, F. (2000) Polarization and interaction of adhesion molecules P-selectin glycoprotein ligand 1 and intercellular adhesion molecule 3 with moesin and ezrin in myeloid cells. *Blood* **95,** 2413–2419
56. Heiska, L., Alfthan, K., Grönholm, M., Vilja, P., Vaheri, A., and Carpén, O. (1998) Association of ezrin with intercellular adhesion molecule-1 and -2 (ICAM-1 and ICAM-2). Regulation by phosphatidylinositol 4,5-bisphosphate. *J. Biol. Chem.* **273,** 21893–21900
57. Iwase, A., Shen, R., Navarro, D., and Nanus, D. M. (2004) Direct binding of neutral endopeptidase 24.11 to ezrin/radixin/moesin (ERM) proteins competes with the interaction of CD44 with ERM proteins. *J. Biol. Chem.* **279,** 11898–11905
58. Mori, T., Kitano, K., Terawaki, S., Maesaki, R., Fukami, Y., and Hakoshima, T. (2008) Structural basis for CD44 recognition by ERM proteins. *J. Biol. Chem.* **283,** 29602–29612
59. Takai, Y., Kitano, K., Terawaki, S., Maesaki, R., and Hakoshima, T. (2008) Structural basis of the cytoplasmic tail of adhesion molecule CD43 and its binding to ERM proteins. *J. Mol. Biol.* **381,** 634–644
60. Terawaki, S., Kitano, K., and Hakoshima, T. (2007) Structural basis for type II membrane protein binding by ERM proteins revealed by the radixin-neutral endopeptidase 24.11 (NEP) complex. *J. Biol. Chem.* **282,** 19854–19862
61. Weinman, E. J., Hall, R. A., Friedman, P. A., Liu-Chen, L. Y., and Shenolikar, S. (2006) The association of NHERF adaptor proteins with G protein-coupled receptors and receptor tyrosine kinases. *Annu. Rev. Physiol.* **68,** 491–505
62. Voltz, J. W., Weinman, E. J., and Shenolikar, S. (2001) Expanding the role of NHERF, a PDZ-domain containing protein adapter, to growth regulation. *Oncogene* **20,** 6309–6314
63. Kim, M., Jiang, L. H., Wilson, H. L., North, R. A., and Surprenant, A. (2001) Proteomic and functional evidence for a P2X7 receptor signalling complex. *EMBO J.* **20,** 6347–6358
64. Gu, B. J., Saunders, B. M., Jursik, C., and Wiley, J. S. (2010) The P2X7-nonmuscle myosin membrane complex regulates phagocytosis of nonopsonized particles and bacteria by a pathway attenuated by extracellular ATP. *Blood* **115,** 1621–1631
65. Adlerz, L., Holback, S., Multhaup, G., and Iverfeldt, K. (2007) IGF-1-induced processing of the amyloid precursor protein family is mediated by different signaling pathways. *J. Biol. Chem.* **282,** 10203–10209
66. Jacobsen, K. T., Adlerz, L., Multhaup, G., and Iverfeldt, K. (2010) Insulin-like growth factor-1 (IGF-1)-induced processing of amyloid-β precursor protein (APP) and APP-like protein 2 is mediated by different metalloproteinases. *J. Biol. Chem.* **285,** 10223–10231
67. Kommaddi, R. P., Thomas, R., Ceni, C., Daigneault, K., and Barker, P. A. (2011) Trk-dependent ADAM17 activation facilitates neurotrophin survival signaling. *FASEB J.* **25,** 2061–2070
68. Le Gall, S. M., Maretzky, T., Issuree, P. D., Niu, X. D., Reiss, K., Saftig, P., Khokha, R., Lundell, D., and Blobel, C. P. (2010) ADAM17 is regulated by a rapid and reversible mechanism that controls access to its catalytic site. *J. Cell Sci.* **123,** 3913–3922
69. Suzuki, T., and Nakaya, T. (2008) Regulation of amyloid β-protein precursor by phosphorylation and protein interactions. *J. Biol. Chem.* **283,** 29633–29637
70. Colombo, A., Bastone, A., Ploia, C., Sclip, A., Salmona, M., Forloni, G., and Borsello, T. (2009) JNK regulates APP cleavage and degradation in a model of Alzheimer's disease. *Neurobiol. Dis.* **33,** 518–525
71. Lee, M. S., Kao, S. C., Lemere, C. A., Xia, W., Tseng, H. C., Zhou, Y., Neve, R., Ahlijanian, M. K., and Tsai, L. H. (2003) APP processing is regulated by cytoplasmic phosphorylation. *J. Cell Biol.* **163,** 83–95
72. Feyt, C., Pierrot, N., Tasiaux, B., Van Hees, J., Kienlen-Campard, P., Courtoy, P. J., and Octave, J. N. (2007) Phosphorylation of APP695 at Thr668 decreases γ-cleavage and extracellular Aβ. *Biochem. Biophys. Res. Commun.* **357,** 1004–1010
73. Schettini, G., Govoni, S., Racchi, M., and Rodriguez, G. (2010) Phosphorylation of APP-CTF-AICD domains and interaction with adaptor proteins: signal transduction and/or transcriptional role—relevance for Alzheimer pathology. *J. Neurochem.* **115,** 1299–1308
74. Stanasila, L., Abuin, L., Diviani, D., and Cotecchia, S. (2006) Ezrin directly interacts with the α_{1b}-adrenergic receptor and plays a role in receptor recycling. *J. Biol. Chem.* **281,** 4354–4363
75. Cant, S. H., and Pitcher, J. A. (2005) G protein-coupled receptor kinase 2-mediated phosphorylation of ezrin is required for G protein-coupled receptor-dependent reorganization of the actin cytoskeleton. *Mol. Biol. Cell* **16,** 3088–3099